

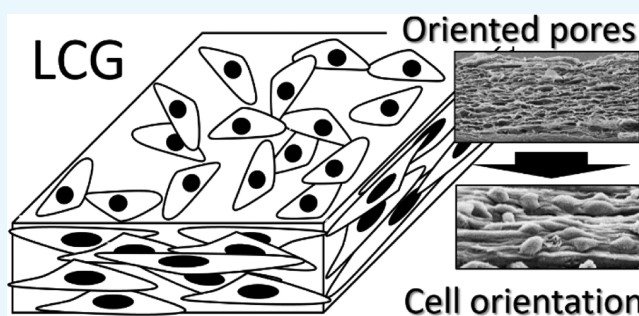
Surface-Selective Control of Cell Orientation on Cyanobacterial Liquid Crystalline Gels

Saranyoo Sornkamnerd,¹ Maiko K. Okajima, Kazuaki Matsumura,¹ and Tatsuo Kaneko^{*,†}

Graduate School of Advanced Science and Technology, Japan Advanced Institute of Science and Technology (JAIST), 1-1 Asahidai, Nomi, Ishikawa 923-1292, Japan

Supporting Information

ABSTRACT: Liquid crystalline hydrogels (LCGs) with layer structures and oriented pores were created using sacran which is a cyanobacterial heteropolysaccharide possessing functional sulfate, carboxylate, and amide groups in common with glycosaminoglycan. The LCG biocompatibility with L929 mouse fibroblasts was confirmed under the appropriate conditions. Enhanced growth and proliferation of L929 cells without exhibiting any toxicity were confirmed. The water contact angle and protein adsorption ability on the LCG were well-controlled by the cross-linking degree. Additionally, fibroblasts were finely oriented on the LCG side face where layer edges made a striped morphology on its surface, whereas the flat top faces of the LCG did not induce any specific cell orientation.



INTRODUCTION

Hydrogels are three-dimensional polymer networks capable of absorbing a large amount of biological liquids such as water or saline while maintaining their structural similarity.^{1,2} They can be applied in a variety of fields such as cell carriers,^{3–5} drug delivery,^{6,7} and engineering scaffolds^{8–10} if they have biological compatibility¹¹ and good cellular function.^{12–15} Cell controllable scaffolds are important biomaterials which lead to the next-generation field of tissue engineering. Elements of the scaffold architecture such as pore size, porosity, pore interconnectivity, and media permeability are key factors in controlling cell activity.^{16,17}

Previously, we prepared tough and porous hydrogels, in which interconnected pores resembling tunnels were perforated only in the side faces, by using the bioderived megamolecule, sacran,¹⁸ which is an exopolysaccharide ($M_w = 1.6 \times 10^7$ g/mol),^{19,20} extracted from *Aphanotheca sacrum* cyanobacteria (Figure S1). Sacran is mainly composed of sugar residues of Glc, Gal, Man, Xyl, Rha, and Fuc and functional monosaccharides such as uronic acids and *N*-acetylated amino sugars, some of which are sulfonated. As a result, sacran has functional groups of carboxyls, sulfates, and amides, which is similar to glycosaminoglycan (GAG). GAG exists in the extracellular matrix and directly attaches to cell surfaces in animal tissues.²¹ Similarly, sacran chains surround *A. sacrum* cells as a main constituent of the extracellular matrix. Thus, we believe that the sacran hydrogels were proper candidates for scaffold constituents.

Herein, we exploited the opportunity to use sacran hydrogels in the tissue engineering field and found that L929 mouse fibroblasts were well-extended on the hydrogels. In addition, we

showed a face-selective cell orientation on the sacran liquid crystalline hydrogel (LCG).

RESULTS AND DISCUSSION

Surface Properties. Sacran LCG scaffolds were fabricated by using a previously reported method.¹⁸ The sacran liquid crystalline solution (0.5 w/v %) was cast at 60 °C and then thermally cross-linked at 100, 120, and 140 °C. Figure 1 shows the scanning electron microscopy (SEM) images of the films, revealing the layered pattern on the side faces yet no specific patterns on the top faces of the films. Afterward, the films were swollen in distilled water and freeze-dried to form porous structures (Figure 1: inset). The pores, which were found in the SEM images of the side faces but not in those of the top faces, were interconnected along the direction of the layers like tunnels. The shape of the surface was analyzed using ImageJ software, which revealed the space between layers as 65 ± 21 , 20 ± 3 , and 11 ± 2 μm for samples cross-linked at 100, 120, and 140 °C, respectively. However, the pore sizes were 26, 19, and 9 μm for those samples.¹⁸

Water contact angle (WCA) was measured to evaluate the wettability on the top surface of dry porous scaffolds. Wettability is an important characteristic of scaffolds and is used to investigate cell behaviors on the materials.²² From the literature, moderate wettability ($\sim 50^\circ$) of the surface from hydrophobicity to hydrophilicity is preferred for the adhesion of cells.²³ Figure 2a shows that the WCA of the scaffold cross-

Received: December 20, 2017

Accepted: February 27, 2018

Published: June 19, 2018

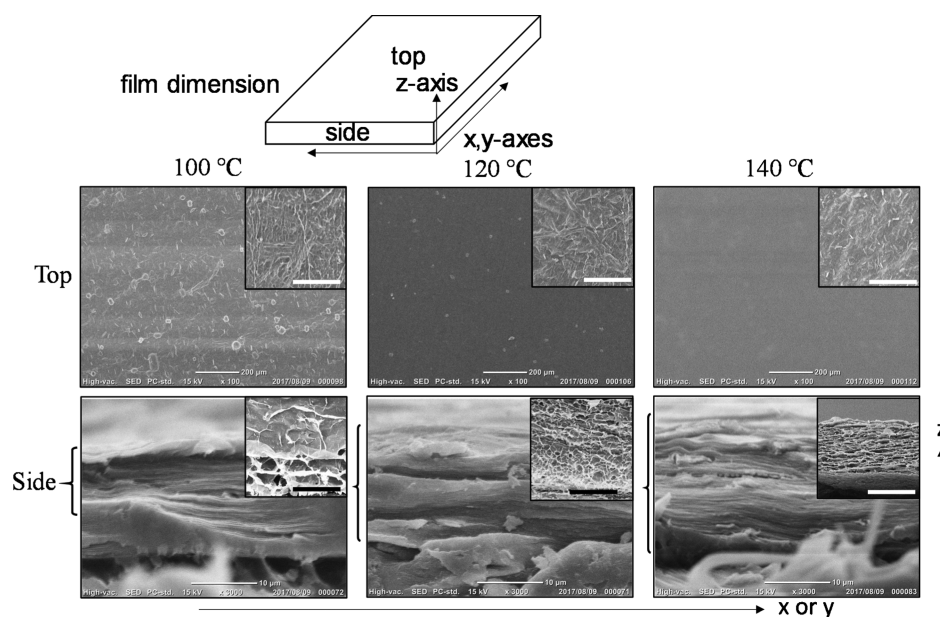


Figure 1. SEM images of layered films (whose dimension shown above images) prepared by casting of 0.5 w/v % sacran solution and annealed at 100, 120, and 140 °C. Images revealed layered patterns on side faces, whereas no specific pattern on the top face. Inset: Porous scaffolds prepared by freeze-drying of layered films (scale bars in insets: 200 μm).

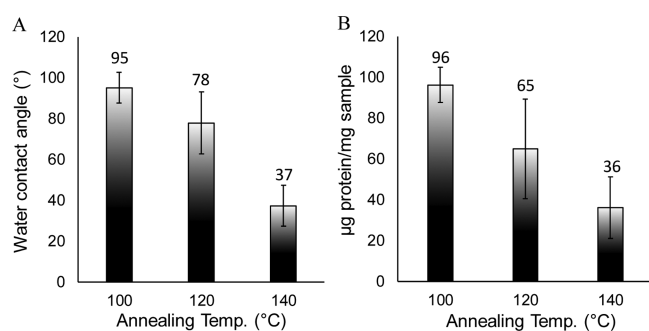


Figure 2. Surface properties of LCG scaffolds which were prepared by freeze-drying of hydrogels from the films thermally annealed at 100, 120, and 140 °C. (A) WCAs on the x - y surface of scaffolds. (B) Protein adsorption degree to scaffolds (mg/mg) after 24 h application. Values are averaged data ($n = 5$), and error bars refer to standard deviation.

linked at 100 °C showed the highest value (95°) and gradually decreased down to 78° for the cross-linking treatment at 120 °C. On the other hand, the WCA was drastically reduced to 37° for the 140 °C treatment. Even though the side surface impacted to cell adhesion, small thickness cannot measure the WCA. The thicknesses were 476 ± 14 , 454 ± 46 , and 242 ± 8 μm for annealing temperatures at 100, 120, and 140 °C, respectively. The result indicated that the hydrophilicity of the LCG surface increased with an increase in the annealing temperature might be attributed to the loss of hydroxyls and carboxyls by thermal esterification as demonstrated previously.^{18,24} These results indicated that the surface wettability of the sacran scaffold could be simply controlled by changing the cross-linking temperature. Moreover, as seen in the SEM images in Figure 1, the top surface of the film was smoother when the annealing temperature was higher. The surface profile was analyzed from SEM images using the ImageJ software result in Figure S2. The surface of LCG scaffolds cross-linked at 100 °C has the highest frequency that refers to the roughness.

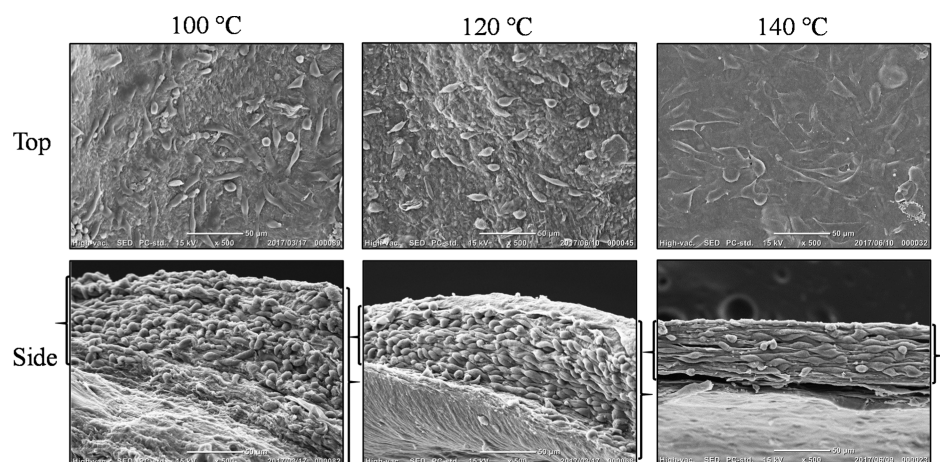


Figure 3. SEM images of L929 fibroblasts taken after incubation for 3 days on LCG scaffolds, which were annealed at 100, 120, and 140 °C.

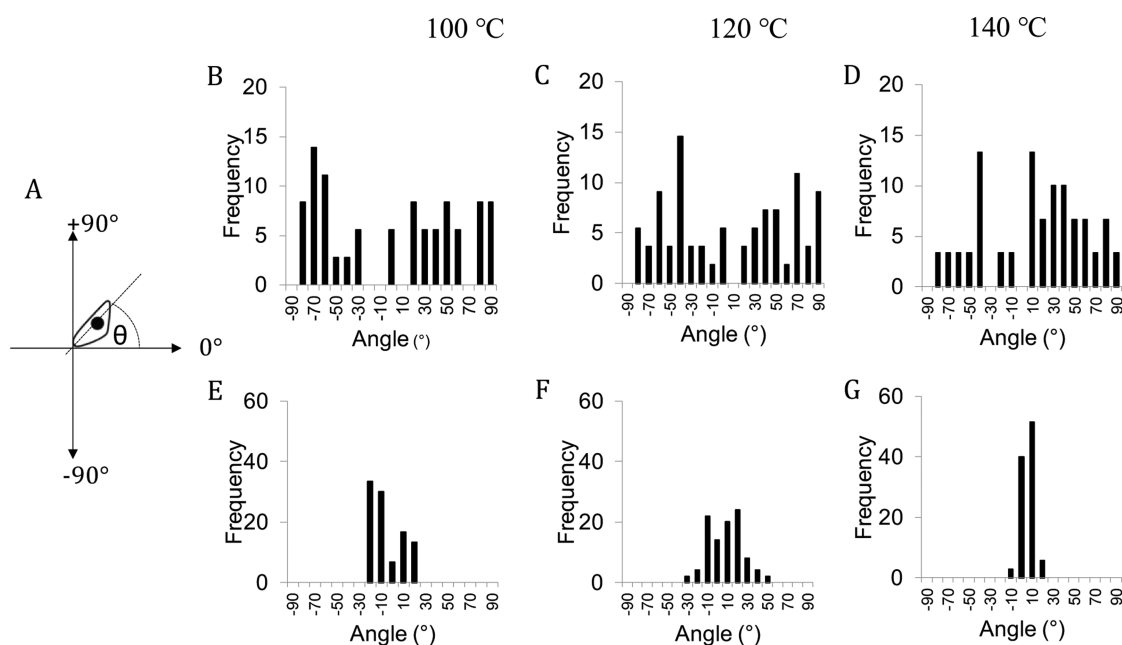


Figure 4. Frequency distribution of the longitudinal direction angle of extended cells to the x -axis (or y -axis) on LCG scaffolds annealed at 100, 120, and 140 °C. (A) Schematic illustration of cell distribution. (B–D) revealed the random distribution of cells on the top surface of LCG scaffolds annealed at 100, 120, and 140 °C, respectively, whereas (E–G) were unidirectional orientation of cell on the side surface of those sample.

The surface profile became smoother on the surface of the samples cross-linked at 120 and 140 °C. In reality, it was difficult for water droplets to remain still at a point on the film annealed at 140 °C²⁵ which was the smoothest scaffold.

Adsorption capability of serum proteins to sacran chains has a vital role in scaffolds because fibronectin, a presentative protein, has a function of promoting cell adhesion and of reorganizing the actin filaments.²⁶ Figure 2b shows the protein adsorption degree ($\mu\text{g}/\text{mg}$) to the sacran LCG. The amount of adsorbed protein was decreased as the cross-linking temperature increased because of the LCG morphology. The LCG prepared after film annealing at a higher temperature had a smaller pore size and lower porosity and had a smaller amount of free functional groups such as hydroxyls and carboxyls which can efficiently bind with protein.²⁷ This result provided important evidence of the control of cell activity on the sacran LCG as a tissue engineering scaffold.

Cell Cultivation. The ability of scaffolds to control cell adhesion and proliferation is crucial for tissue engineering applications. L929 mouse fibroblasts were used to evaluate the cell–matrix interaction in the sacran LCG. After cell cultivation, we took SEM images of cells on the LCG to evaluate the cell compatibility of the sacran scaffolds (Figure 3). SEM images demonstrated that a number of cells were attached to both the top and side surfaces of the scaffolds and exhibited an elongated shape, revealing the good biocompatibility of sacran LCG scaffolds. This observation was supported by the live and dead assay using fluorescent microscopy (Figure 4). The fluorescent image of fibroblast L929 cells after 72 h incubation showed that almost all of the cells were colored green, that is, alive, and only a few were red, that is, dead, strongly suggesting the high cell compatibility of the sacran chains. The cell viability was detected by a Cell Counting Kit-8 (CCK-8) to characterize the proliferation of L929 cells on the sacran scaffolds. Figure S4a shows the absorbance values obtained after 3 days of incubation. At the first day of cell culture, the number of cells on scaffolds increased with an increase in the annealing

temperature of the precursor films from 100 to 140 °C. After 2 days of incubation, the number of cells on the scaffold was increased but the values showed a peak at an annealing temperature of 120 °C. The number of cells on the scaffold from the film annealed at 140 °C was lower after 3 days of incubation, presumably because of excessive hydrophobicity of the samples at 140 °C. In addition, the particularly narrow area of the side surface and low protein adsorption ability might be related to the low number of cells adhered to the samples at 140 °C. As a whole, the LCG scaffolds from the sacran films annealed at 100 and 120 °C were more suitable for cell cultivation than the LCG from the film annealed at 140 °C. Figure S4b shows the density of cells on the top and side surfaces of the LCG, analyzed using SEM images (Figure 3) of cells on the scaffolds cultured for 3 days. The density of cells on the top surface was higher than that on the side surface for all three samples. However, the cell density on the top surface correlates well with the protein adsorption degree on the scaffolds in Figure 2b. Although the side surface area was smaller than the top, the number of cells on the side was affected. Because of the porous morphology of materials, the rough surface was the main condition for cell adhesion, thus many cells attached onto the side surface.²⁸ Furthermore, the tendency of protein adsorption corresponded to the number of attached cells.

The morphology of cells attached on the top and side surfaces was different. On the side surface, cells were extended along layers of the LCG scaffolds, indicating that the surface structure of the LCG materials can play a significant role in the cell attachment and proliferation.²⁹ To quantify the orientation of L929 cells in response to the layered structure of the LCG scaffolds, we analyzed the angle of the extension direction of cells to the central line between the top and bottom edges of the side surface as a reference, from SEM images in Figure 3. The orientation angle ranged from -90° to $+90^\circ$ and an orientation angle of 0° represent parallel alignment to the reference line. Figure 4 demonstrates that almost all of the cells

on the side surfaces were within $\pm 30^\circ$, meaning good orientation behavior. On the other hand, L929 cells were randomly extended on the top surface because of the LCG scaffolds not presenting any directing morphology guiding the cell alignment. The orientation degree increased with the annealing temperature of the precursor films; 63% of cells aligned finely within $\pm 15^\circ$ on the LCG from the film annealed at 100 °C, whereas the figure was 80% at 120 °C and 92% at 140 °C. This tendency of layer structural ordering is in agreement with a previous report.¹⁸ Then, the increase in the annealing temperature created the sacran scaffolds with a high orientation of layer stripes to introduce efficiently the orientation of fibroblast cells. These results revealed that cell orientation behavior was well-controlled by the layer structure, selectively on the side surface. These unique characteristics of the sacran LCG scaffold may lead to the oriented organization of artificial tissue.

CONCLUSIONS

It was demonstrated that the sacran LCG scaffolds with an anisotropic porous structure were excellent materials for tissue engineering applications. They showed a layered pattern on pores which could guide the cell adhesion behavior. Surface properties such as the WCA presented the proper condition from 95 to 37°. Proteins were well bound to the sacran LCG surfaces presumably owing to the chemical structure including functional groups such as hydroxyls and carboxyls. Both the WCA and protein adsorption were controlled by the thermal cross-linking temperature. We can speculate that the sacran scaffolds had good biocompatibility thanks to their structural similarity to GAG in native tissue. The most important function of the sacran LCG is that induction of fibroblast orientation on the side surface having layer edges and the orientation can be controlled by changing the hydrogel preparation condition. Thus, sacran porous LCG materials have good biocompatibility and are promising biomaterials for tissue engineering scaffolds.

MATERIALS AND METHODS

Materials. Sacran was dedicated from Green Science Materials Inc. (Kumamoto, Japan) and used as received.

LCG Scaffold Fabrication. LCGs were prepared by freeze-drying of hydrogels which were fabricated by the solvent casting process as reported before.¹⁸ Briefly, 50 mL of 0.5 w/v % sacran solution was casted on a polypropylene case ($50 \times 50 \times 50 \text{ mm}^3$) and dried in an oven at 60 °C for 24 h to form translucent films. The films were thermally treated at 100, 120, and 140 °C, for 6 h to cross-link the sacran chains in a dry film state. When the films were immersed in deionized water at room temperature for 24 h, they became equilibrium-state hydrogels. Next, sacran hydrogels were frozen by keeping in liquid nitrogen for about 10 min and then drying in a freeze-drying apparatus (EYELA, FDU-1200) for 72 h to form LCG scaffolds.

Characterization of Sacran Scaffolds. To investigate the surface morphology, the microscopy images were examined using SEM (JEOL, JCM-6000PLUS). The samples were mounted onto metal stubs using a carbon tape. The stubs were then coated with gold using a sputter coater machine. Then, the ImageJ software was used to analyze the surface profile and the space between layers.

The WCA experiment of the sacran scaffolds was performed on the top surface using a contact angle meter (Drop Master, Kyowa Interface Science Co., Ltd., Japan) at room temperature.

To measure the protein adsorption, LCG scaffolds were placed in a 96-well plate having Dulbecco's modified Eagle's medium (DMEM) + 10% fetal bovine serum (FBS) and were incubated at 37 °C for 24 h. After incubation, the scaffolds were washed with phosphate-buffered saline (PBS) solution thrice. The washed scaffolds were then incubated with the 2 w/v % sodium dodecyl sulfate solution (Wako, Japan) at room temperature for 3 h. Total protein was calculated using the bicinchoninic acid assay.³⁰

Cell Culture. A mouse fibroblast-like cell line (L929) was selected for all biological assays to evaluate the biocompatibility and cell adhesion behavior on LCG scaffolds. The L929 fibroblast cell line was obtained from the American Type Culture Collection (Manassas, VA). The cells were cultured in the DMEM (Sigma, USA) supplemented with 10% heat-inactivated FBS (Biocrom AG, Germany) incubated at 37 °C in a humidified atmosphere with 5% CO₂.

Cell Adhesion. Prior to biological assays, all LCG scaffolds were sterilized under UV radiation overnight²⁸ and then immersed in ethanol 70% (v/v) for 3 days. Subsequently, 1 mL of $1.0 \times 10^5 \text{ cells mL}^{-1}$ cell suspension was seeded on each LCG scaffolds and cultured for 1, 2, and 3 days at 37 °C. After each incubation period, the samples were rinsed with a buffer saline (PBS, Sigma-Aldrich, USA). The number of cells adhering to the scaffold was then counted.

Proliferation Assay.³¹ CCK-8 (Dojindo, Japan) was applied to evaluate the cell number according to the manufacturer's instruction. Each LCG, after rinse with PBS, was incubated in 0.1 mL of the growth medium supplemented with 10 μL of CCK-8 stock solution for 3 h at 37 °C in a humidified atmosphere of 5% CO₂ in air. The absorbance at 450 nm was measured.

Cell Morphology. The morphology of the cultured L929 ($1.0 \times 10^5 \text{ cell/scaffold}$) was observed by SEM images. After 3 days of culture, the cells were fixed by 10% formalin neutral buffer solution (Wako, Japan) for 24 h. The dehydration process was performed on each specimen in ethanol (60, 70, 80, 90, 100, and 100%) and two times of *t*-butanol, each for 1 h, which is then dried at room temperature. After that, they were sputter-coated with gold and viewed by SEM. The orientation degree of extended cells was measured using ImageJ software. A reference line was set along the central line of upper and lower edges in an SEM image, and then the orientation angle to the reference line was evaluated.³²

Live/Dead Assay.^{9,31} Cell viability in sacran LCG scaffolds was evaluated using the live/dead assay. Constructs were harvested, gently rinsed twice with PBS, and then incubated with calcein AM and ethidium homodimer-1 (EthD-1) for 15 min to stain live (green) and dead (red), respectively, for 15 min at 37 °C and 5% CO₂ humidified incubator. Samples were viewed using a fluorescence microscope (BZ-X700, KEYENCE).

ASSOCIATED CONTENT

Supporting Information

The Supporting Information is available free of charge on the ACS Publications website at DOI: 10.1021/acsomega.7b02027.

Surface roughness; chemical structure of polymer; live/dead assay of fibroblast L929 cells; and cell proliferation and cell density (PDF)

AUTHOR INFORMATION

Corresponding Author

*E-mail: kaneko@jaist.ac.jp. Phone: +81-761-51-1631. Fax: +81-761-51-1635 (T.K.).

ORCID

Saranyoo Sornkamnerd: 0000-0002-1929-5406

Kazuaki Matsumura: 0000-0001-9484-3073

Present Address

[†]Energy and Environment Area, School of Materials Science, Graduate School of Advanced Science and Technology, Japan Advanced Institute of Science and Technology (JAIST), 1-1 Asahidai, Nomi, Ishikawa 923-1292, Japan (T.K.).

Author Contributions

S.S. designed the experiment and wrote the paper; K.M. interpreted the cell culture data; M.K.O. extracted the sacran, and T.K. supervised and set the scientific aims. All authors contributed to the results, conception, and presentation of the data.

Notes

The authors declare no competing financial interest.

ACKNOWLEDGMENTS

This work was supported by a grant-in-aid for Challenging Exploratory Research of MEXT (16K14077).

REFERENCES

- Xiang, H.; Xia, M.; Cunningham, A.; Chen, W.; Sun, B.; Zhu, M. Mechanical properties of biocompatible clay/P(MEO2MA-co-OEGMA) nanocomposite hydrogels. *J. Mech. Behav. Biomed. Mater.* **2017**, *72*, 74–81.
- Yang, Y.; Wang, C.; Wiener, C. G.; Hao, J.; Shatas, S.; Weiss, R. A.; Vogt, B. D. Tough Stretchable Physically-Cross-linked Electrospun Hydrogel Fiber Mats. *ACS Appl. Mater. Interfaces* **2016**, *8*, 22774–22779.
- Wang, Z.; Wang, J.; Jin, Y.; Luo, Z.; Yang, W.; Xie, H.; Huang, K.; Wang, L. A Neuroprotective Sericin Hydrogel As an Effective Neuronal Cell Carrier for the Repair of Ischemic Stroke. *ACS Appl. Mater. Interfaces* **2015**, *7*, 24629–24640.
- Jain, M.; Matsumura, K. Polyampholyte- and nanosilicate-based soft bionanocomposites with tailorable mechanical and cell adhesion properties. *J. Biomed. Mater. Res., Part A* **2016**, *104*, 1379–1386.
- Jain, M.; Matsumura, K. Thixotropic injectable hydrogel using a polyampholyte and nanosilicate prepared directly after cryopreservation. *Mater. Sci. Eng., C* **2016**, *69*, 1273–1281.
- Xue, B.; Kozlovskaya, V.; Liu, F.; Chen, J.; Williams, J. F.; Campos-Gomez, J.; Saeed, M.; Kharlampieva, E. Intracellular Degradable Hydrogel Cubes and Spheres for Anti-Cancer Drug Delivery. *ACS Appl. Mater. Interfaces* **2015**, *7*, 13633–13644.
- Zhang, Z.; He, Z.; Liang, R.; Ma, Y.; Huang, W.; Jiang, R.; Shi, S.; Chen, H.; Li, X. Fabrication of a Micellar Supramolecular Hydrogel for Ocular Drug Delivery. *Biomacromolecules* **2016**, *17*, 798–807.
- Kim, M.; Hong, B.; Lee, J.; Kim, S. E.; Kang, S. S.; Kim, Y. H.; Tae, G. Composite System of PLCL Scaffold and Heparin-Based Hydrogel for Regeneration of Partial-Thickness Cartilage Defects. *Biomacromolecules* **2012**, *13*, 2287–2298.
- Mohanty, S.; Alm, M.; Hemmingsen, M.; Dolatshahi-Pirouz, A.; Trifol, J.; Thomsen, P.; Dufva, M.; Wolff, A.; Emnéus, J. 3D Printed Silicone–Hydrogel Scaffold with Enhanced Physicochemical Properties. *Biomacromolecules* **2016**, *17*, 1321–1329.
- Yan, H.; Saiani, A.; Gough, J. E.; Miller, A. F. Thermoreversible Protein Hydrogel as Cell Scaffold. *Biomacromolecules* **2006**, *7*, 2776–2782.
- Anderson, J. M.; Rodriguez, A.; Chang, D. T. Foreign body reaction to biomaterials. *Seminars in Immunology*; Elsevier, 2008; pp 86–100.
- Ovsianikov, A.; Deiwick, A.; Van Vlierberghe, S.; Dubruel, P.; Möller, L.; Dräger, G.; Chichkov, B. Laser fabrication of three-dimensional CAD scaffolds from photosensitive gelatin for applications in tissue engineering. *Biomacromolecules* **2011**, *12*, 851–858.
- Gupta, P.; Vermani, K.; Garg, S. Hydrogels: from controlled release to pH-responsive drug delivery. *Drug Discovery Today* **2002**, *7*, 569–579.
- Van Vlierberghe, S.; Vanderleyden, E.; Dubruel, P.; De Vos, F.; Schacht, E. Affinity study of novel gelatin cell carriers for fibronectin. *Macromol. Biosci.* **2009**, *9*, 1105–1115.
- Patel, M.; Kaneko, T.; Matsumura, K. Switchable release nano-reservoirs for co-delivery of drugs via a facile micelle–hydrogel composite. *J. Mater. Chem. B* **2017**, *5*, 3488–3497.
- Peltola, S. M.; Melchels, F. P. W.; Grijpma, D. W.; Kellomäki, M. A review of rapid prototyping techniques for tissue engineering purposes. *Ann. Med.* **2008**, *40*, 268–280.
- Yeong, W.-Y.; Chua, C.-K.; Leong, K.-F.; Chandrasekaran, M. Rapid prototyping in tissue engineering: challenges and potential. *Trends Biotechnol.* **2004**, *22*, 643–652.
- Sornkamnerd, S.; Okajima, M. K.; Kaneko, T. Tough and Porous Hydrogels Prepared by Simple Lyophilization of LC Gels. *ACS Omega* **2017**, *2*, 5304–5314.
- Okajima, M. K.; Kaneko, D.; Mitsumata, T.; Kaneko, T.; Watanabe, J. Cyanobacteria That Produce Megamolecules with Efficient Self-Orientations. *Macromolecules* **2009**, *42*, 3057–3062.
- Okajima, M. K.; le Nguyen, Q. T.; Tateyama, S.; Masuyama, H.; Tanaka, T.; Mitsumata, T.; Kaneko, T. Photoshrinkage in polysaccharide gels with trivalent metal ions. *Biomacromolecules* **2012**, *13*, 4158–4163.
- Chi, L.; Wolff, J. J.; Laremore, T. N.; Restaino, O. F.; Xie, J.; Schiraldi, C.; Toida, T.; Amster, I. J.; Linhardt, R. J. Structural Analysis of Bikunin Glycosaminoglycan. *J. Am. Chem. Soc.* **2008**, *130*, 2617–2625.
- Song, W.; Mano, J. F. Interactions between cells or proteins and surfaces exhibiting extreme wettabilities. *Soft Matter* **2013**, *9*, 2985–2999.
- Lee, J. H.; Lee, J. W.; Khang, G.; Lee, H. B. Interaction of cells on chargeable functional group gradient surfaces. *Biomaterials* **1997**, *18*, 351–358.
- Okajima, M. K.; Mishima, R.; Amornwachirabodee, K.; Mitsumata, T.; Okeyoshi, K.; Kaneko, T. Anisotropic swelling in hydrogels formed by cooperatively aligned megamolecules. *RSC Adv.* **2015**, *5*, 86723–86729.
- Spori, D. M.; Drobek, T.; Zürcher, S.; Ochsner, M.; Sprecher, C.; Mühlebach, A.; Spencer, N. D. Beyond the Lotus Effect: Roughness Influences on Wetting over a Wide Surface-Energy Range. *Langmuir* **2008**, *24*, 5411–5417.
- Kim, H.-W.; Kim, H.-E.; Salih, V. Stimulation of osteoblast responses to biomimetic nanocomposites of gelatin–hydroxyapatite for tissue engineering scaffolds. *Biomaterials* **2005**, *26*, 5221–5230.
- Jin, J.; Jiang, W.; Yin, J.; Ji, X.; Stagnaro, P. Plasma proteins adsorption mechanism on polyethylene-grafted poly(ethylene glycol) surface by quartz crystal microbalance with dissipation. *Langmuir* **2013**, *29*, 6624–6633.
- Yang, A.; Huang, Z.; Yin, G.; Pu, X. Fabrication of aligned, porous and conductive fibers and their effects on cell adhesion and guidance. *Colloids Surf., B* **2015**, *134*, 469–474.
- Peter, M.; Ganesh, N.; Selvamurugan, N.; Nair, S. V.; Furuike, T.; Tamura, H.; Jayakumar, R. Preparation and characterization of chitosan–gelatin/nanohydroxyapatite composite scaffolds for tissue engineering applications. *Carbohydr. Polym.* **2010**, *80*, 687–694.
- Deepthi, S.; Jeevitha, K.; Nivedhitha Sundaram, M.; Chennazhi, K. P.; Jayakumar, R. Chitosan–hyaluronic acid hydrogel coated

poly(ϵ -caprolactone) multiscale bilayer scaffold for ligament regeneration. *Chem. Eng. J.* **2015**, *260*, 478–485.

(31) Zhao, Y.; Tan, K.; Zhou, Y.; Ye, Z.; Tan, W.-S. A combinatorial variation in surface chemistry and pore size of three-dimensional porous poly(ϵ -caprolactone) scaffolds modulates the behaviors of mesenchymal stem cells. *Mater. Sci. Eng., C* **2016**, *59*, 193–202.

(32) McCormick, A. M.; Maddipatla, M. V. S. N.; Shi, S.; Chamsaz, E. A.; Yokoyama, H.; Joy, A.; Leipzig, N. D. Micropatterned Coumarin Polyester Thin Films Direct Neurite Orientation. *ACS Appl. Mater. Interfaces* **2014**, *6*, 19655–19667.